

Superhydrophobic behaviour of modified AA6082 alloy surfaces

L. Calabrese, A. Khaskhoussi, E. Proverbio

Three different approaches were applied to obtain textured superhydrophobic surfaces on Al6082 aluminium alloys (boiling water, HF/HCl and HNO₃/HCl concentrated solution etching). Afterwards, an octadecylsilane thin film was deposited on all as-treated surfaces to reduce their surface energy. The morphological analysis showed that a specific dual nano/micro-roughness structure was obtained for each pre-treated surface. All samples evidenced a superhydrophobic behaviour, with water contact angle (WCA) in the range 160°-180°. The adhesion force between the water droplets and superhydrophobic surfaces were evaluated. The results evidenced that HF/HCl etched samples showed the lowest adhesion and highest WCA. Furthermore, the relationship among hydrophobic behaviour, corrosion resistance and surface morphology was discussed comprehensively.

KEYWORDS: ALUMINIUM ALLOY, SUPERHYDROPHOBIC SURFACE, CORROSION RESISTANCE, ADHESION FORCE, COATING.

INTRODUCTION

Recently, super-hydrophobic textured surfaces were extensively investigated due to their advantages in specific application fields where anti-icing and self-cleaning properties and high corrosion resistance are required [1, 2]. According to the lotus effect, superhydrophobic behaviour is greatly exalted by coupled micro and nano hierarchical textures so that water droplets can not wet the surface but simply roll off and spontaneously remove the dirt particles on leaf surface. That would suggest new and innovative strategies designing an effective super-anti wetting material by controlling surface engineering properties [3]. In such a context, functional superhydrophobic surfaces can be obtained coupling hierarchical rough surface morphology with low surface energy materials. Several surface engineering approaches were applied in order to obtain low energy superhydrophobic surfaces on aluminium alloy substrates. Nevertheless, their industrial implementation was always limited because of high processing times and costs. In such a context, new synthesis techniques able to lead to super-hydrophobic surfaces by easy to use, cost-effective and environmentally friendly approaches are developed. Chen et al. [4] applied chemical etching to induce a super-hydrophobic behaviour on aluminium alloy surfaces. Analogously, Ruan et al. [5] investigated the effect of different process parameters on chemical etching and surface hydrophobization, evidencing that an optimal parameter selection is a key factor to obtain high performing surfaces with hydrophobic or super-hydrophobic behaviour. Guo et al. [6] obtained superhydrophobic aluminium surface developing a two steps method. However, although relevant research improve-

ments have been made in this field, it is still pending the issue to optimize low energy superhydrophobic aluminium surfaces by using a simple, time-saving and environment-friendly manufacturing procedure. At the same time, the improvement in knowledge, to better define the relationship between hierarchical textured morphology and superhydrophobic surface performances, is required.

Luigi Calabrese, Edoardo Proverbio

Department of Engineering, University of Messina, Messina, Italy

Amani Khaskhoussi

Department of Engineering, University of Messina, Messina, Italy - National Interuniversity Consortium of Materials Science and Technology, INSTM, Firenze, Italy

MATERIALS AND METHODS

An EN AW-6082 T6 aluminium alloy substrates (30 mm × 24 mm × 2 mm) preliminarily, were ultrasonically cleaned with ethanol, acetone and ultra-pure water and finally dried at room temperature in a silica-gel dryer. In order to create hierarchical rough structure, three different surface pre-treatment procedures were applied: i) Ultra-pure boiling water treatment for 5 min, ii) HNO₃/HCl chemical etching (volume ratio 1:3) in ultra-pure water solution for 1 hour, iii) HF/HCl chemical etching (73% HCl, 5% HF, 22% ultra-pure water) for 15s. Afterwards, the etched samples were cleaned in an ultrasonic bath with ultra-pure water to remove residuals acids and dried at 70° for 60 min. Then, the resulting aluminium substrates were immersed for 10 min in 1 wt.% solution of

Octadecyltrimethoxysilane (S18) in toluene. Eventually, all substrates were treated for 3 h at 100 °C to complete the silane curing. In Table 1, the as-prepared sample details are summarized.

Static water contact angles (WCA) were measured by an Attention Theta Tensiometer equipment (with Biolin Scientific) at room temperature. Fifty water contact angle measurements (droplets volume 3 µl) were performed for characterization. Morphological analysis of textured surface was carried out by using a focused ion dual beam/scanning electron microscope (FIB-SEM ZEISS Crossbeam 540). Roughness details of the surfaces were acquired by performing AFM maps obtained by a VEECO Explorer microscope.

Tab. 1 - Sample details

Code	Surface Treatment	Silane
AR	--	--
AR-S	--	S18
Al-BW	Boiling water	--
Al-BWS	Boiling water	S18
Al-HF	HF/HCl solution	--
Al-HFS	HF/HCl solution	S18
Al-HN	HNO ₃ /HCl solution	--
Al-HNS	HNO ₃ /HCl solution	S18

RESULTS AND DISCUSSION

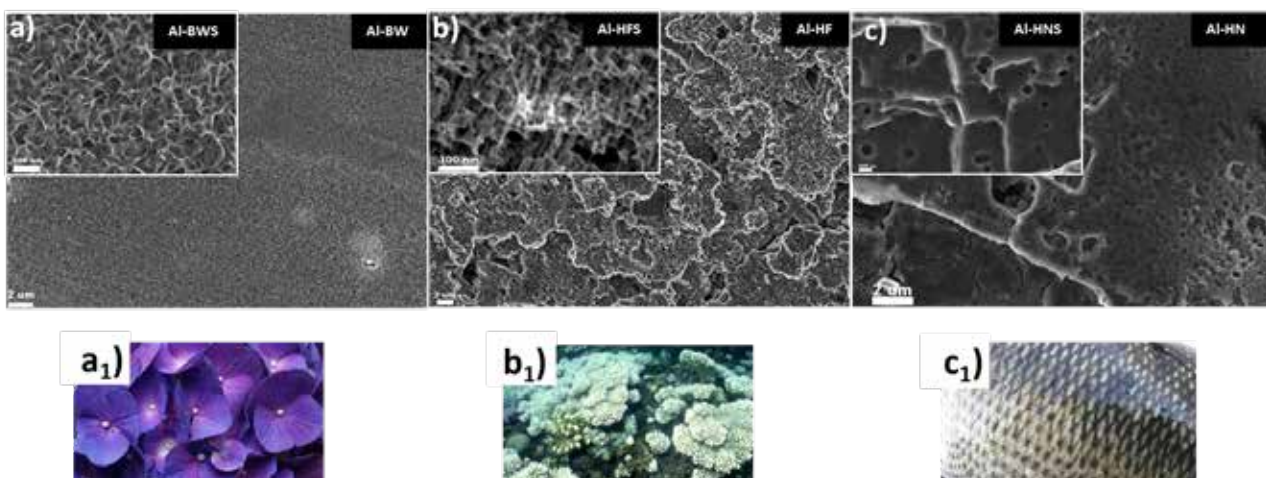


Fig. 1 - SEM micro-graphs of (a) Al-BW and Al-BWS (; (b) Al-HF and Al-HFS, (c) Al-HN and Al-HNS

Fig. 1 shows the surface morphology of all batches. In the upper left corner the surface morphology after the silanization step. All coatings have a quite homogeneous structure. Although, depending on the applied etching process different surface textures can be identified. In particular:

- Boiling H₂O: the surface morphology appears as a flower-like structure with several petal-like flakes (thickness 30 nm) randomly overlapped each other, generating a complex micro and nanoscale upper-structure. This structure is due to the formation of a barrier oxy/hydroxide layer constituted mainly by an amorphous or pseudo-amorphous boehmite (AlO(OH).H₂O) [7].
- HF/HCl: Bimodal structure was observed on the surface of treated aluminium. Micro-structure: is like a coral network structure with the presence of micro large deeper attack zones. Nano-structure is similar to a pixel like structure with clear edges and corners. Only on this surface it was possible to observe by SEM the presence of the octadecylsilane film located mainly on the profile asperities.
- HNO₃/HCl: This surface is characterized by a micro-scale (platelets like fish scales) and nano-scale (regular small pits) bimodal structure. This texture meaningfully increases the effective surface area and the roughness surface profile. Several pits (diameter about 150 nm) randomly growth on the smooth platelets (sides about 2-4 μm). This peculiar morphology was due to aluminium grain orientation, preferred dissolution planes and secondary phases distribution that favour local acid etching promoting the micro/nano-scale bimodal structure on the aluminium alloy surface. The AA6082 alloy is indeed characterized by Fe-Mn inclusions with dimensions in the range 5-8 μm,

randomly distribute [8]. Furthermore, several dislocations and crystal defects cause the presence of areas more sensitive to the acidic etching solution than other metal surface zones[9].

To better evaluate the morphology and roughness profiles of the surface, AFM scanning was performed on all batches. Fig. 2 shows 3D AFM maps (sides 5×5 μm²). Furthermore, statistical analysis of roughness profile was carried out to quantitatively compare the three surface modification approaches. Ra (arithmetic average height) and Rq (root mean square roughness) parameters are reported in the topside of each image. The 3D AFM topographic images for the three surface pre-treated samples are morphologically compatible with SEM morphology identified in Fig. 1. Fig. 2a shows the surface topography of Al-BW sample. Spheroidal shaped asperities randomly located on the surface can be identified. This morphology can be related to the observed flower-like colonies of boehmite flakes. The gap between peaks and valleys in the Al-BW sample is about 300-400 nm. Instead the root width of each flower-like cluster is very small (~ 100 nm). Fig. 2b shows the surface morphology of the Al-HF sample. The presence of large high and depressed areas can be identified. Furthermore, several asperities due to pixel-like blocks are distinguished, inducing a very high roughness profile, both a micro and nano level. Finally, Fig. 2c, is related to the surface morphology observed on Al-HN sample. At microlevel, flat and smooth platelets are evident. Very few and randomly located nano-asperities can be furthermore identified. constituted by some platelets at micro level and some asperities located at nanoscale level. The structure although evidently rough, can be identified as a jagged plateau with some steps.

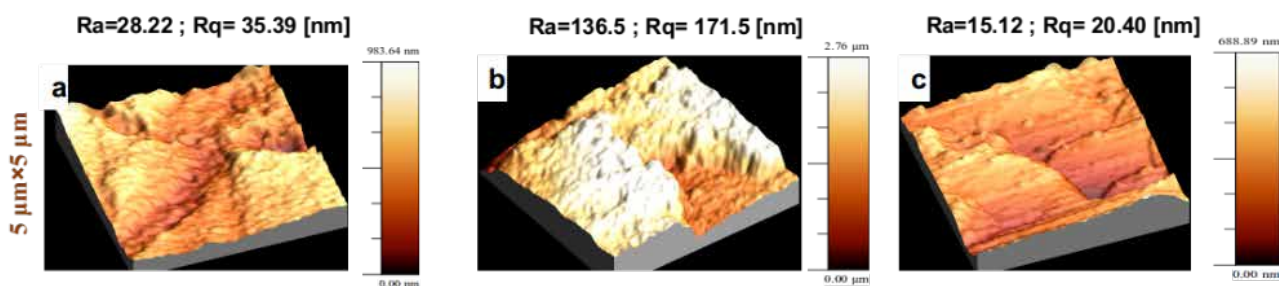


Fig. 2 - 3D AFM map on the 5×5 μm² surface of a) Al-BW; b) Al-HF and c) Al-HN samples

Al-HF sample shows a nano surface roughness (Ra=136.5 nm, Rq=171.5 nm) about six times higher than Al-BW and Al-HN samples (Ra=28.22 and Rq=35.39 nm; Ra=15.12 nm and Rq=20.40 nm respectively) highlighting that the etching treatment with HF/ HCl solution induced a stronger roughening effect than the others approaches.

In order to assess the relationship between hydrophobic behaviour, surface energy and surface treatment on the aluminium alloy support, Fig. 3 shows the average water contact angle (WCA)

for as-received before and after S18 deposition (AR and AR-silane, respectively) and all surface modified superhydrophobic samples. The surface wettability is strongly affected by both surface energy and surface morphology. Due to the surface roughening step the contact angle of AR substrate decreases of about 40° (from 68.7±2.9° to <25°). Afterwards, the silanization step a significant decrease of surface energy is induced as evidenced by the strongly superhydrophobic behaviour (WCA >150°) evidenced for all samples after S18 deposition.

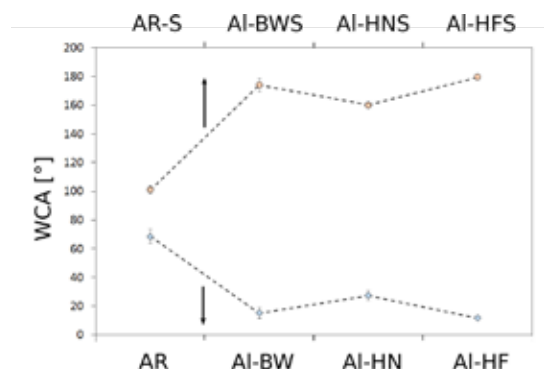


Fig. 2 - Contact angle for distilled water on surface treated and untreated aluminium alloy substrate before silanization step (bottom X axis) and after silanization dip-coating process (top X axis).

The combined effect of surface treatment and silanization induces a relevant increase of the WCA. In fact, the surface behaviour of AR sample, after the deposition of the S18 silane films, evolves from hydrophilic to hydrophobic. The water contact angle increases from $68.7 \pm 2.9^\circ$ to $101 \pm 2.9^\circ$. Applying the same silanization step on the etched aluminium alloy surfaces a further significant increase in the WCA can be highlighted. The best result was observed for AI-HFS sample, where average WCA of around 180° was observed. Also AI-HNS and AI-BWS samples showed average WCA above 150° ($\sim 160^\circ$ and $\sim 174^\circ$, respectively).

It is worth of noting that, although all samples evidenced water contact angles above the threshold of 150° , only AI-HFS sample evidenced a very low rolling angle (i.e. $< 5^\circ$). This result suggests that for this sample Cassie-Baxter regime in the interaction with water droplet could occur. In particular, thanks to the synergistic effect of micro/nano roughness and low surface energy induced by S18 upper layer, air pockets can remain entrapped on the profile asperities exalting the hydrophobic behaviour of the surface, according to Cassie-Baxter rule. At the same time, the presence of air pocket entrapped at the water/solid interface reduces the interfacial adhesion of the water droplet with the substrate favouring a lower rolling angle.

Instead the AI-HWS and AI-HNS samples showed an opposite behaviour with very high rolling angle. These surfaces are characterized by a Wenzel state wettability behaviour, where water droplet fully penetrates the surfaces asperities without air pockets in grooves.

The so prepared superhydrophobic surfaces with controllable water adhesion can be used in wide range of applications. The low water adhesion surfaces, such as AI-HFS where low rolling angle was observed, can be used for several industrial applications where self-cleaning, anti-icing, anti-bioadhesion and anti-corrosion performances are required. While, the superhydrophobic but highly adhesive surface, such as AI-BWS, can be used as a safe and economic support for high-cost

and rare drugs transportation (e.g. anti-cancer drugs delivery in human body) [10].

In order to assess the superhydrophobic behaviour of energy modified Al6082 surfaces some further consideration concerning the interaction of the modified surface with silane compound to obtain the low energy silane layers can be argued. The octadecyl-silane compound can form three covalent bond oxygen bridges with the substrate due to the interaction of the high reactive silanol groups (Si-OH) with the aluminium hydroxyl groups (Al-OH), obtaining Al-O-Si bonds at the metal/silane interface. That leads to a compact and adherent film on the metal substrate [11]. Instead the long polymer chain of the silane compounds is not able to react and it forms an organic well ordered external surface monolayer, characterized by high hydrophobic properties. In fact, the silane monolayer structure has a preferential orientation of the hydrophobic alkyl chains, that induces an improvement of the hydrophobic performances of the coating surface [12]. This behaviour can be suitably designed using long alkyl chains molecules that are able to acquire a regular and oriented arrangement, thank to long induced dipole formation that favours an electrostatic interaction among [13].

Instead the surface hydrophobization is avoided when limited accessible sites on the substrate are able to interact with the silane compound, leading to a more disordered layer with less effective hydrophobic performances [14]. Therefore, in such a context, the surface morphology is an important factor that need to be taken into account to effectively tailor superhydrophobic low energy surfaces by silanization.

In particular, concerning the experience reported in this work, for sample with only nanometric roughness (A-W sample) the silane coating can be deposited mainly on the peaks and on sporadic large cavities, exalting the surface asperities and therefore the Cassie-Baxter contribute to hydrophobic behaviour of the coating. Conversely for samples with a smoother surface (A-N sample) the silane will cover mainly the large valleys thus reducing the surface roughness, limiting the con-

tribute of the structure to the super-hydrophobic behaviour. Instead, on a surface with micro- and nano-roughness profiles, as in A-F sample, a reliable synergistic effect on hierar-

chical rough surface occurred obtaining a compact and well distributed silane layer leading to the very high water contact angle observed.

SUMMARY

In summary, superhydrophobic Al surface with controlled wetting behaviour, water adhesion and corrosion resistance were effectively prepared by using a cost-effective and flexible approaches. A two steps procedure was applied: a short term treatment with boiling water, or HF/HCl or HNO₃/HCl concentrated etching solution, followed by an in situ polymerization of an octadecylsilane layer on all samples. The superhydrophobic aluminium surfaces have been characterized by SEM,

AFM, contact angle measurements. All surfaces evidenced a superhydrophobic behaviour. The higher contact angle was achieved by HF/HCl treatment. A synergetic effect of low surface energy and bimodal rough profile was defined as a key role to obtain high performing anti-corrosion superhydrophobic surfaces. These results are promising for further development and research improvements in order to better assess the relationship among hierarchical morphology, low energy surface and super-hydrophobicity.

REFERENCES

- [1] Liu M, Zheng Y, Zhai J et al. Bioinspired Super-antiwetting Interfaces with Special Liquid-Solid Adhesion. *Acc. Chem. Res.* 2010; 43(3):368–377.
- [2] Liu K, Zhang M, Zhai J et al. Bioinspired construction of Mg-Li alloys surfaces with stable superhydrophobicity and improved corrosion resistance. *Appl. Phys. Lett.* 2008; 92(18):1–4.
- [3] Cheng Z, Du M, Lai H et al. From petal effect to lotus effect: A facile solution immersion process for the fabrication of super-hydrophobic surfaces with controlled adhesion. *Nanoscale* 2013; 5(7):2776–2783.
- [4] Chen Z, Guo Y, Fang S. A facial approach to fabricate superhydrophobic aluminum surface. *Surf. Interface Anal.* 2010; 42(1):1–6.
- [5] Ruan M, Li W, Wang B et al. Optimal conditions for the preparation of superhydrophobic surfaces on Al substrates using a simple etching approach. *Appl. Surf. Sci.* 2012; 258(18):7031–7035.
- [6] Guo Y, Wang Q, Wang T. Facile fabrication of superhydrophobic surface with micro/nanoscale binary structures on aluminum substrate. *Appl. Surf. Sci.* 2011; 253(13):5831–5836.
- [7] Geiculescu AC, Strange TF. A microstructural investigation of low-temperature crystalline alumina films grown on aluminum. *Thin Solid Films* 2003; 426(1–2):160–171.
- [8] Calabrese L, Bruzzaniti P, Proverbio E. Pitting corrosion of aluminum alloys in anhydrous ethanol. *Mater. Corros.* 2018; 69(12):1815–1826.
- [9] Zhang Y, Wu J, Yu X, Wu H. Low-cost one-step fabrication of superhydrophobic surface on Al alloy. *Appl. Surf. Sci.* 2011; 257(18):7928–7931.
- [10] Yohe ST, Herrera VLM, Colson YL, Grinstaff MW. 3D superhydrophobic electrospun meshes as reinforcement materials for sustained local delivery against colorectal cancer cells. *J. Control. Release* 2012; 162:92–101.
- [11] van Ooij WJ, Zhu D, Stacy M et al. Corrosion Protection Properties of Organofunctional Silanes—An Overview. *Tsinghua Sci. Technol.* 2005; 10(6):639–664.
- [12] Calabrese L, Bonaccorsi L, Capri A, Proverbio E. Effect of silane matrix composition on performances of zeolite composite coatings. *Prog. Org. Coatings* 2016; 101:100–110.
- [13] Calabrese L, Bonaccorsi L, Capri A, Proverbio E. Effect of silane matrix on corrosion protection of zeolite based composite coatings. *Metall. Ital.* 2014; 106(6):35–39.
- [14] Calabrese L, Bonaccorsi L, Capri A, Proverbio E. Electrochemical behavior of hydrophobic silane-zeolite coatings for corrosion protection of aluminum substrate. *J. Coatings Technol. Res.* 2014; 11(6):883–898.